A Single-Fiber Bi-Directional WDM Self-Healing Ring Network with Bi-Directional OADM for Metro-Access Applications

Xiaofeng Sun, *Student Member, IEEE,* Chun-Kit Chan, *Senior Member, IEEE,* Zhaoxin Wang, *Student Member, IEEE,* Chinlon Lin, *Fellow, IEEE,* and Lian-Kuan Chen, *Senior Member, IEEE*

***Abstract*— We propose and demonstrate a single-fiber bi-directional wavelength division multiplexing self-healing ring network for metro-access applications. By incorporating a simple bi-directional optical add-drop multiplexer at each network node as well as employing our proposed alternate-path switching scheme, the bi-directional traffic can be restored promptly under single fiber failure in the ring network. All the protection switching is performed at the hub only, thus the operation, administration and management cost can be easily optimized.**

***Index Terms*— Optical networks, bi-directional transmission, optical add-drop multiplexer, wavelength division multiplexing, network protection.**

I. INTRODUCTION

WAVELENGTH division multiplexing (WDM) technology is promising to offer cost-effective access of high-bandwidth data in optical fiber. With the recent significant advances in wavelength routing devices and optical switches, it is feasible to perform wavelength routing and switching optically. Hence, reconfigurable WDM networks have emerged as a viable approach to support high capacity metropolitan area applications. To assure reliable data delivery, network survivability is a crucial issue in network design. Any failures in network links or components would lead to huge loss in data or even business. To facilitate effective and prompt network protection and restoration, it is highly desirable to perform network survivability in the optical layer. Conventionally, network protection schemes for optical WDM ring networks were similar to the SONET self-healing rings (SHRs) [1], in which duplicated protection fibers were employed to provide redundant paths, and the line or path protection switching was incorporated at the hub and the network nodes. Several proposals [1]-[4] on optical protection rings including dedicated protection rings and shared protection rings have been reported for both optical channel layer and optical multiplex section layer. However, they required at least two working fiber paths to support the protection function. Several other self-healing ring networks have been demonstrated previously. In [5], a dense-WDM self-healing ring network, with a unidirectional optical add-drop multiplexer (OADM), which was based on acousto-optic switches, at each network node, was proposed. In [6], optical filters and optical switches were employed at the access nodes for wavelength dropping and protection switching, respectively. In [7]-[8], an array waveguide grating (AWG) add-drop filter was employed as the OADM and a loop back circuit was implemented to provide protection switching at each access node. However, these approaches still required two working fiber paths to support both protection as well as bi-directional transmission. In order to further reduce the system cost and increase the fiber efficiency in SHR networks, single-fiber bi-directional SHR networks based on bi-directional optical add-drop multiplexer (B-OADM) [9]-[11] have recently attracted much research interest. However, these B-OADMs were mostly based on AWG multiplexers, which may induce high insertion loss and complexity. As the OADM will be dropping and adding one or just a few wavelength channels, simple B-OADM is highly desirable. In [12], a simple four-port B-OADM, which was basically a Mach-Zehnder interferometer with identical fiber Bragg gratings on its arms (MZI-FBG), was proposed. It could be employed to drop and add one designated wavelength channel from the optical ring network.

In [13], we have proposed and demonstrated a new single-fiber bi-directional WDM SHR metro-access ring network, comprising a hub node and multiple access nodes (ANs). Although the physical network is a single-fiber ring network, the logical connections between the hub node and the access nodes are actually in star configuration, via designated wavelengths. Thus, all data traffic collected from all ANs is terminated and routed to the outside network through the hub node. Each AN is incorporated with a simple and low-cost B-OADM, which is based on MZI-FBG, for adding/dropping wavelength channels to/from the hub node. By making use of the spectral periodicity of the $N \times 2$ AWG at the hub node, a novel wavelength assignment plan is proposed to facilitate both the bi-directional data transmission as well as the proposed alternate-path switching scheme for protection against any single fiber failure in the network. All the protection switching is performed at the hub only, the operation, administration and management cost can be easily optimized. The proposed ring network can realize traffic restoration without the need of any extra protection fiber nor doubling the number of optical transceivers. In addition, in this paper, we further provide an optimization of the B-OADM at the access nodes, based on

Manuscript received September 5, 2005; revised November 29, 2006. This work was partially supported by a research grant from the Research Grants Council of Hong Kong SAR, China (Project No. CUHK4216/03E).

The authors are with the Lightwave Communications Laboratory, Department of Information Engineering, The Chinese University of Hong Kong, Shatin, N.T., HONG KONG (email: ckchan@ie.cuhk.edu.hk).

Digital Object Identifier 10.1109/JSAC-OCN.2007.023305.

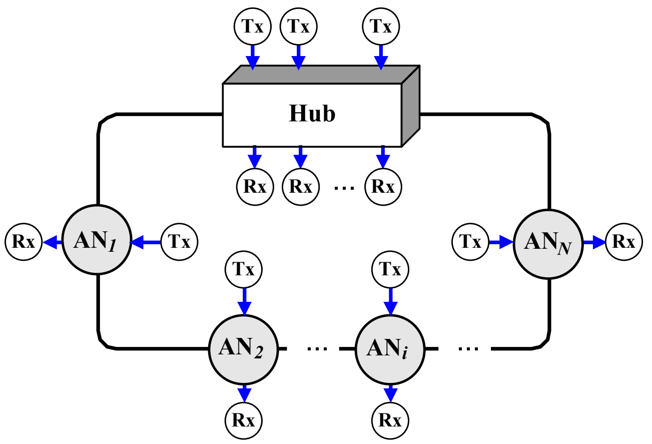

Fig. 1. Single-fiber bidirectional metro-access ring with four ANs.

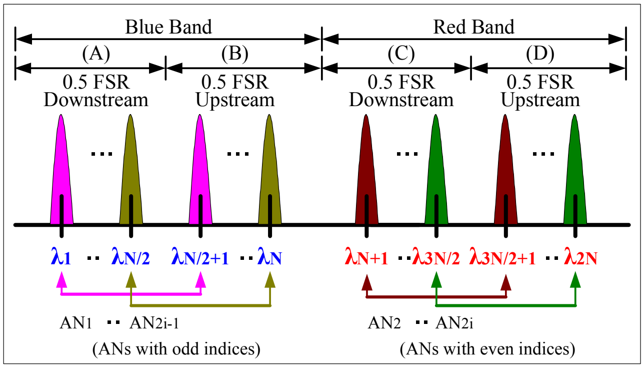

Fig. 2. Proposed wavelength assignment plan. FSR: free-spectral range of AWG; N: number of wavelengths in one free-spectral range of AWG.

the power budget analysis. In order to illustrate the scalable design of our proposed network, we will provide the design for the hub node and the access nodes when a larger number of access nodes are supported.

This paper is organized as follows. Section II describes the proposed network architecture and the structure of the B-OADM. Besides, the operation principles of the proposed alternate-path switching scheme for protection against any single fiber failure will be illustrated. Section III describes the experimental demonstration and measurements to prove the effectiveness of the proposed network architecture and protection scheme. Section IV discusses the optimization of the access nodes as well as the network scalability. Section V summaries the paper.

II. Network Architecture and Node Structure

Fig. 1 shows our proposed single-fiber bi-directional metro-access network with one hub node and N ANs. The ANs (AN_1 to AN_N) with ascending indices are arranged in counter-clockwise direction along the single-fiber ring. Each node is equipped with one pair of downstream receiver and upstream transmitter; while the hub node has N pairs of downstream transmitters and upstream receivers. Therefore, altogether $2N$ wavelengths are required. All data traffic collected from all ANs is terminated and routed through the hub node. Fig. 2 illustrates the proposed wavelength assignment plan. For index $i = 1, \ldots, N/2$, the wavebands A (λ_i) and B ($\lambda_{N/2+i}$) in the blue band are allocated for the downstream and the upstream wavelength channels of the ANs with odd indices (AN_{2i-1}), respectively, while the wavebands C (λ_{N+i}) and D ($\lambda_{3N/2+i}$) in the red band are for the downstream and the upstream wavelength channels of the ANs with even indices (AN_{2i}), respectively. Besides, wavelength λ_k ($k = 1, \ldots, N$) is separated from λ_{N+k} by one free-spectral range (FSR) of the AWG at the hub node; while the upstream and the downstream wavelengths assigned to each AN are separated by half of the FSR. Equivalently, for $k = 1, \ldots, N$; AN_k with odd k is assigned with $\lambda_{(k+1)/2}$ and $\lambda_{(N+k+1)/2}$ as the downstream and the upstream wavelengths, respectively; while AN_k with even k is assigned with $\lambda_{(2N+k)/2}$ and $\lambda_{(3N+k)/2}$ as the downstream and the upstream wavelengths, respectively. For instance, for a four-node (N=4) network with eight wavelength channels (λ_1 to λ_8), the designated (downstream(D), upstream(U)) wavelength pair for AN_1, AN_2, AN_3 and AN_4 are (D=λ_1, U=λ_3), (D=λ_5, U=λ_7), (D=λ_2, U=λ_4), and (D=λ_6, U=λ_8), respectively (see Fig. 4(a)). Note that λ_l, is one FSR away from λ_5; and so are the wavelength pairs (λ_2, λ_6), (λ_3, λ_7), and (λ_4, λ_8). Besides, λ_1 is half of an FSR away from λ_3; and so are the wavelength pairs (λ_2, λ_4), (λ_5, λ_7), and (λ_6, λ_8). Under normal operation, each of the downstream wavelengths originated from the hub node is destined for its respective ANs in either clockwise (CW) or counter-clockwise (CCW) direction, whichever having the smallest number of hops. In contrast, each of the upstream wavelengths from each AN traverses towards the hub node in both CW and CCW directions.

The block diagram of the B-OADM at AN_k is shown in Fig. 3(a). The upstream wavelength λ_u ($u = (N + k + 1)/2$ for odd k or $u = (3N + k)/2$ for even k) is added and transmitted to the hub node in both CW and CCW directions; while the downstream wavelength λ_d ($d = (k + 1)/2$ for odd k or $d = (2N + k)/2$ for even k) originating from either CW or CCW direction is dropped and transmitted to the receiver. Figs. 3(b) and 3(c) show the two possible configurations of the B-OADM for an AN with odd index, for example. The first one (Fig. 3(b)) is based on a Mach-Zehnder interferometer with identical fiber Bragg gratings on its arms (MZI-FBG) [12]. The upstream signal is added through the two optical couplers and transmitted to the hub node in both CW and CCW directions; while the downstream signal originating from either CW or CCW direction is dropped by the MZI-FBG and transmitted to the downstream receiver via an optical coupler. The MZI-FBG determines the dropped downstream wavelength, whereas the rest of other downstream wavelengths will simply bypass the AN. The second configuration (Fig. 3(c)) is based on a four-port thin-film filter, which is used to simultaneously add and drop the upstream and the downstream wavelengths, respectively. Besides, other alternative B-OADMs could also be used as long as the add-drop functions described in the block diagram of Fig. 3(a) can be achieved.

Fig. 4(a) shows the network architecture and the hub node structure of the proposed single-fiber ring network with four nodes, i.e. $N = 4$, for example, with eight wavelength channels (λ_1 to λ_8). The hub node consists of an $N \times 2$ ($N = 2^n$) AWG and M ($M \leq N$) transceivers. Each transceiver, designated for a particular AN, is associated with a 2×2 optical switch and a Blue/Red filter. Every two

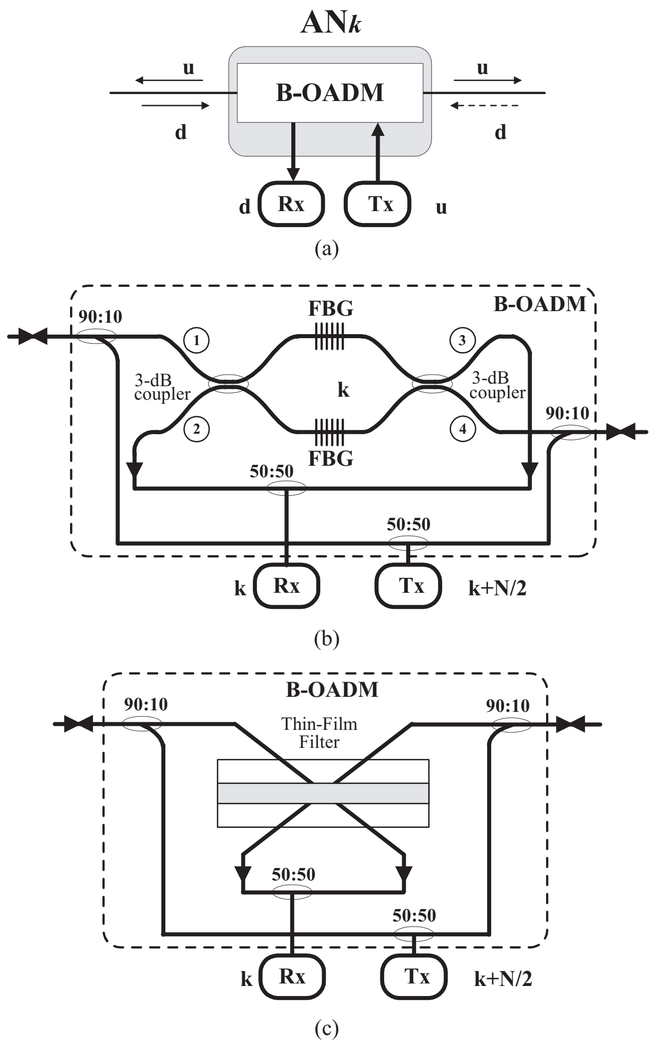

Fig. 3. (a) Block diagram of the proposed B-OADM at AN_k. λ_u is the upstream wavelength ($u = (N + k + 1)/2$ for odd k or $u = (3N + k)/2$ for even k); λ_d is the downstream wavelength ($d = (k + 1)/2$ for odd k or $d = (2N + k)/2$ for even k). Note that λ_d reaches AN_k in either direction (solid or broken-line arrow) which has the shortest path from the hub only. (b) Configuration of the MZI-FBG based B-OADM. (c) Configuration of the thin-film filter based B-OADM .

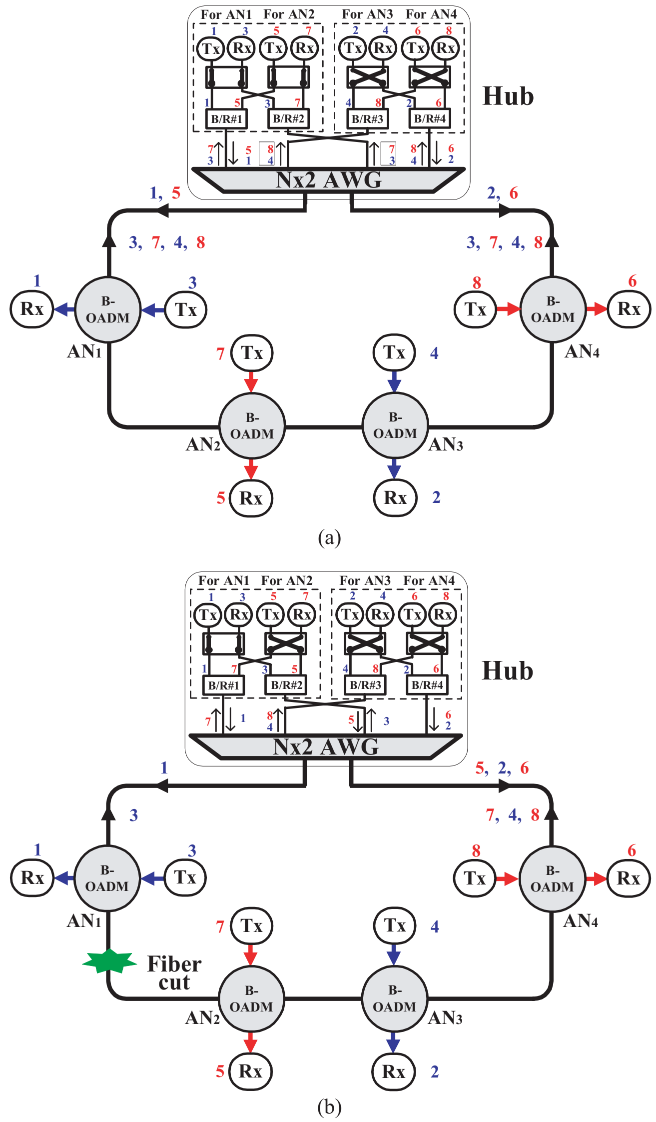

Fig. 4. Configuration of the proposed single-fiber bidirectional metro-access network under (a) normal operation mode. B/R: Blue/Red band filter. Note: the upstream wavelength channels marked with boxes are the working ones; while those without boxes will be blocked by their respective destined transmitters. (b) Protection mode. Note: λ_5 (downstream) is re-routed to the clockwise direction of the ring network while λ_7 (upstream) is selected from the counter-clockwise direction.

adjacent transceivers form a group and communicate with their respective ANs, one with odd index $(2i - 1)$ and the other with even index $(2i)$, respectively, for $i = 1, \ldots, N/2$. Under normal operation, the 2×2 optical switches associated with AN_1, AN_2, ..., $AN_{N/2}$ are in bar states; while those associated with $AN_{N/2+1}$, $AN_{N/2+2}$, ..., AN_N are in cross states so as to choose the smaller number of hops for the downstream signals. For AN_{2i-1} (say AN_1), the transmitter with downstream wavelength λ_k (say λ_1) and the receiver with upstream wavelength $\lambda_{N/2+i}$ (say λ_3), both of which are in the blue band, are connected to the respective blue-band ports of the two Blue/Red filters (say B/R#1 and B/R#2) in the same group, respectively, as depicted in Fig. 2 and Fig. 4(a). Similarly, for AN_{2i} (say AN_2), the transmitter with downstream wavelength λ_{N+i} (say λ_5) and the receiver with upstream wavelength $\lambda_{3N/2+i}$ (say λ_7), both of which are in the red band, are connected to the respective red-band ports of the two Blue/Red filters (say B/R#1 and B/R#2) in the same group, respectively. In general, the combined port of the B/R#$(2i - 1)$ (say B/R#1) and that of the B/R#$(2i)$ (say B/R#2) are connected to the i^{th} (say 1^{st}) and the $(N/2 + i)^{th}$ (say 3^{rd}) input ports of the $N \times 2$ (say 4×2) AWG, respectively. The spectral transmission peaks of the two output ports of the AWG are spaced by half of its FSR, and each of them are connected to the transmission fiber of the ring network in either CW or CCW direction. The downstream wavelengths with odd indices (say λ_1, λ_5) and even indices (say λ_2, λ_6) will be propagating in CCW and CW directions in the ring network, respectively. On the other hand, as each AN will send out its upstream wavelength in both directions, thus two copies of the upstream wavelengths (say λ_3, λ_4, λ_7, λ_8) originating from all ANs will reach the $N \times 2$ AWG, where they are demultiplexed and routed towards the respective transceivers at the hub, via the respective Blue/Red filters and 2×2 optical switches. One of the copies of the upstream wavelengths would reach their respective upstream receivers; while the other copy of the upstream wavelengths would reach the transmitters where they would be blocked by the built-in optical isolators of all transmitters at the hub. Fig. 4(a) illustrates the flow of the downstream and the upstream wavelengths under normal operation.

In case of any single fiber cut between any two ANs, some ANs would not be able to receive their downstream wavelengths while the respective upstream receivers of the affected ANs at the hub would not be able to receive their upstream wavelengths. Such conditions will trigger all the 2×2 optical switches associated with the transceivers designated for the affected ANs at the hub to toggle their switching states automatically, either from bar state to cross state or vice versa. As a result, all the blocked downstream wavelengths can be routed to the affected ANs in an opposite propagating direction along the ring network; while all the respective upstream receivers at the hub can still receive a copy of their designated upstream wavelengths. Fig. 4(b) illustrates the flow of the downstream and the upstream wavelengths when the fiber between AN_1 and AN_2 is broken, as an example. Under this condition, the downstream wavelength for AN_2 (λ_5) could not reach AN_2 via the CCW path. Thus the protection switching at the hub re-routes λ_5 to go along the CW path and reach the downstream receiver at AN_2 via the B-OADM. At the same time, the upstream wavelength λ_7 from AN_2 would reach the respective upstream receiver at the hub via a different path, as illustrated in Fig. 4(b). Note that when there is a single fiber cut between $AN_{N/2}$ and $AN_{N/2+1}$ in an N-node ring network for even N, no protection switching is needed as all of the downstream and the upstream wavelengths could still be routed to their respective receivers along their normal paths. With this proposed protection mechanism, a fast 100% restoration of any single fiber cut in the ring network can be achieved and all protection switching operations are performed at the hub only.

III. Experiment & Results

In the experiment, we adopted the B-OADM based on a commercially available MZI-FBG, as shown in Fig. 3(b). We first characterized the performance of the proposed B-OADM. The reflectivity of the FBG in the FBG-MZI was 99.94%. The 3-dB bandwidth of the input-drop and input-bypass transfer functions of the B-OADM was around 0.25 nm, which is determined by the grating design and fabrication, as shown in the Fig. 5(a) and Fig. 5(b), respectively. Thus, the proposed B-OADM is capable of multiplexing/demultiplexing DWDM optical channels with a channel spacing of 0.8 nm. For the dropped signal, there are three types of possible crosstalk. The first one is due to the leakage of the bypass wavelengths (λ_1 to λ_{2N} except λ_k) to the drop port (i.e. from port 1 to $2/3$ and from port 4 to $2/3$). The port numbers are shown in Fig. 3(b). This type of heterodyne crosstalk was measured to be less than -29 dB, as shown in the Fig. 5(c) and could be suppressed by optical filters. The second one is due to the leakage of the dropped wavelength λ_k to the bypass port (i.e. from port 1 to 4 or from port 4 to 1), which is caused by the imperfect reflection of the FBG. This type of crosstalk was measured to be below -30 dB. Since the dropped wavelength λ_k originated from the hub would be transmitted to the AN in either CW or CCW unidirectionally at one time, the residual dropped signal after passing through the B-OADM would not affect the network performance. The last one is due to the leakage of the dropped wavelength λ_k to the drop port on the other side (i.e. from port 1 to 3 and from port 4 to 2). Although this type of homodyne crosstalk could not be filtered off at the receiver, it was measured to be below -40 dB, owing to the interference property of the MZI structure. Thus this had negligible influence on the network performance. For the added signal, since it was added and transmitted to the hub in both CW and CCW directions, its performance was sensitive to the reflection at each B-OADM. The crosstalk level of the reflection of the bypass added signals at the B-OADM (e.g. from port 1 to port 1 or from port 4 to port 4) plus the possible Rayleigh backscattering was measured to be less than -60 dB, such that the transmission performance of the added signal would not be degraded. The receiver sensitivity (at BER = 10^{-9}) was also measured as a function of the misalignment of the dropped wavelength channel from the FBGs' centre wavelength, as shown in Fig. 6. As another signal was added through two separate optical couplers, the added signals would not affect the signal dropped by the MZI-FBG. It showed that the usable bandwidth ($\sim$0.2 nm) was almost the same as the 3-dB bandwidth of the transfer function even with the presence of the added signal. Thus the limit on the usable bandwidth of the conventional configuration of OADM using MZI-FBG for adding and dropping signals at the same time could be alleviated [14].

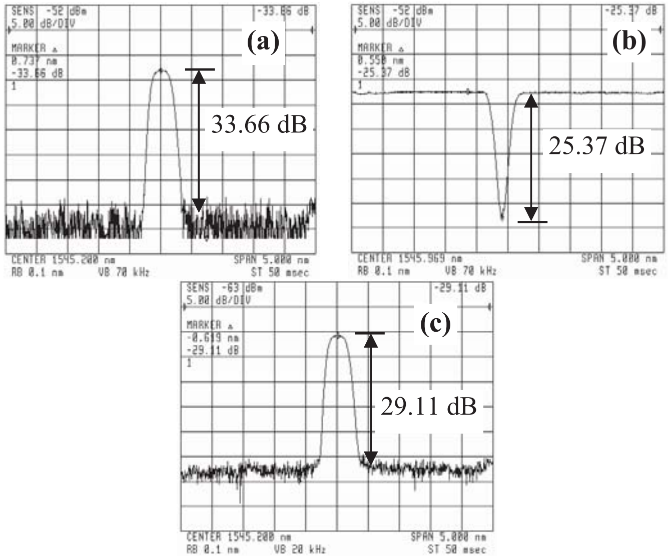

Fig. 5. (a) Input-drop port transfer function of the B-OADM. (b) Input-bypass port transfer function of the B-OADM. (c) Crosstalk level on the dropped signal measured at the port 2 of B-OADM.

We have also experimentally demonstrated the proposed network with one hub node and two ANs. A piece of 10-km conventional single-mode fiber (SMF) was used to connect an AN to the hub or the adjacent AN. At the hub, the Blue/Red filters with 18-nm passband at both blue and red bands were used and connected to a 16×16 AWG, with 100-GHz channel spacing and a FSR of 12.8 nm. The output ports 1 and 9 of the AWG were used to connect to the transmission fibers of the ring network. The wavelengths (downstream; upstream)

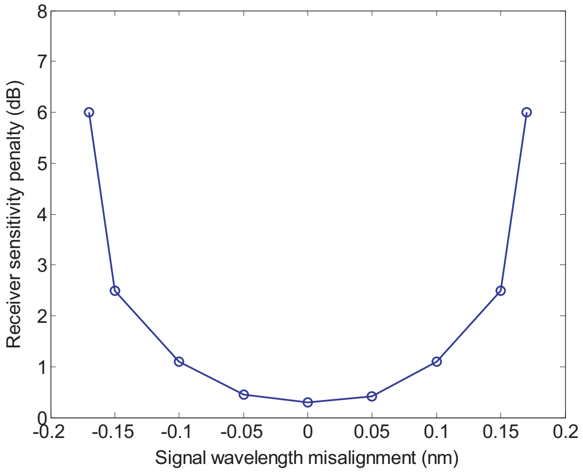

Fig. 6. Receiver sensitivity penalty measured as a function of the fluctuation of the dropped wavelength channel.

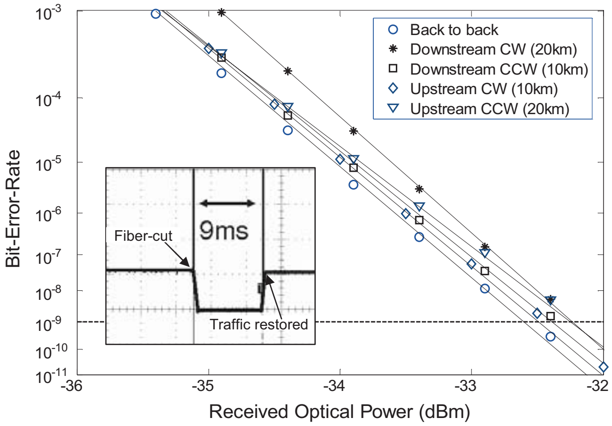

Fig. 7. BER measurement of the traffic between the hub node and AN_1 under operation and protection modes. Inset shows the restoration time measurement under the protection mode. CW: clockwise direction; CCW: counter-clockwise direction.

assigned for AN_1 and AN_2 were (λ_1:1545.2 nm; λ_9:1551.6 nm) and (λ_{17}:1568.0 nm; λ_{25}:1574.4 nm), respectively. Note that the two downstream wavelengths were spaced by one FSR of the AWG and so were the upstream wavelengths. All the wavelengths channels were directly modulated at 2.5 Gb/s (PRBS $2^{31}-1$) and the optical power per channel at the output of the hub was amplified to 0 dBm by an Erbium-doped fiber amplifier (EDFA). At the hub, the wavelengths λ_1 was transmitted to AN_1 in CCW direction; while λ_{17} was transmitted to AN_2 in CW direction. At the same time, two other wavelengths λ_2 (1546.0 nm) and λ_{18} (1568.8 nm) were transmitted in the CW and CCW directions to simulate the downstream signals for AN_2 and AN_4, respectively. At AN_1 the downstream wavelength λ_1 was dropped by the MZI-FBG at the B-OADM; while the upstream wavelength λ_9 was added and transmitted to the hub in both CW and CCW paths. Similarly, at AN_2, the downstream wavelength λ_{17} was dropped by the MZI-FBG at the B-OADM; while the upstream wavelength λ_{25} was added and received by the avalanche photodiode (APD) receivers at the hub. A tap coupler and a monitoring photodiode were employed in front of each upstream receiver at the hub so as to detect any signal loss due to any possible fiber cut in the network.

The bit-error-rate (BER) performance of the 2.5-Gb/s traffic between the hub and AN_1 under both normal and protection modes were measured and were depicted in Fig. 7. In all cases, the measured receiver sensitivities at BER = 10^{-9} were close to each other. The small induced power penalty (< 0.5 dB) compared to the back-to-back measurement was due to possible crosstalk of the MZI-FBG at the B-OADM analyzed above and the chromatic dispersion of fiber. Then, the fiber between the hub and AN_1 was disconnected to simulate the fiber cut. The inset of Fig. 7 shows the downstream power level measured at the receiver at AN_1. The switching time was measured to be about 9 ms and this corresponds to the network traffic restoration time achieved. This switching time greatly depended on the switching response of the electro-mechanical optical switches employed in our experiment. Similar switching waveform was also obtained at the upstream receiver for AN_1 at the hub.

IV. Optimization of Access Node and Network Scalability

In order to estimate the power budget of the proposed network, we optimize the coupling ratio of the optical couplers for adding upstream signals incorporated at each B-OADM. We assume that the output power per channel of the hub is amplified to 0 dBm by a bi-directional EDFA inside the hub, the output power from the transmitter at each AN is 3 dBm, the length of the fiber link between adjacent ANs is 10 km with 2 dB loss, the APD receiver sensitivity is -30 dBm at BER = 10^{-9} at 2.5 Gb/s, and the insertion loss of the MZI-FBG is 0.5 dB. If the coupling ratio of the two couplers for adding upstream signal is $x:(1-x)$, the total insertion loss of the B-OADM at each AN for the bypass, dropped and added signals are $[-20log_{10}(x)+0.5]$ dB, $[-10log_{10}(x)+3.5]$ dB and $[-10log_{10}(1-x)+3]$ dB, respectively. Considering the worst case (under protection mode) with N nodes, both the dropped and the added signals pass through $(N-1)$ ANs to reach the AN and the hub respectively, which experience $[(-20log_{10}(x)+0.5)\cdot(N-1)]$ dB bypass loss plus $2N$ dB transmission loss. Thus we have the following power budget equations,

For dropped signal:

$$[-20log_{10}(x)+0.5]\cdot(N-1)+2N-10log_{10}(x)+3.5=30 \quad (1)$$

For added signal:

$$[-20log_{10}(x)+0.5]\cdot(N-1)+2N-10log_{10}(1-x)+3=33 \quad (2)$$

The number of ANs supported in the network is plotted as a function of the coupling ratio of the optical couplers for adding upstream signals, as depicted in Fig. 8. It shows that the maximum $N=6$ is achieved when x = 0.9. Thus, the coupling ratio of the couplers for adding upstream signals is chosen to be $90:10$; and the proposed network is capable of supporting six ANs without any in-line optical amplifiers.

To further illustrate the scalable design of the proposed network, the general hub configuration which can support N ANs, where N is an even number, is shown in the Fig. 9. There are N transceivers at the hub, each supports its respective AN. Arranged from the left to the right in Fig. 9, the k^{th}

($k = 1, \ldots, N$) transceiver from the left is responsible for AN_k. Each transceiver is accompanied with one 2×2 optical switch and one Blue/Red filter (B/R). An $N \times 2$ AWG is used at the hub for the wavelength multiplexing and routing. Under normal operation, the optical switches for the first $N/2$ transceivers designated for AN_1 to $AN_{N/2}$ are configured to bar state; while those in the last $N/2$ transceivers designated for $AN_{N/2+1}$ to AN_N are configured to cross state. Two adjacent transceivers (say, AN_i and AN_{i+1}, $i = 1, \ldots, N/2$) form a group and communicate with their respective ANs, one with odd index $(2i-1)$ and the other with even index $(2i)$, respectively. At the i^{th} group, the Blue/Red filter with odd index $(2i-1)$ is connected to the i^{th} input port of the $N \times 2$ AWG; while the Blue/Red filters with even index $(2i)$ is connected to the $(N/2+i)^{th}$ input port of the $N \times 2$ AWG. That is, the Blue/Red filters with odd indices and even indices are connected to the first half (i.e. Ports 1 to N) and the second half (i.e. Ports $N/2+1$ to N) of the AWGs input ports, respectively. The spectral transmission peaks of the two output ports of the AWG are spaced by half of its FSR. Each of these two output ports is connected to the transmission fiber of the ring network in either direction. Besides, in case of the number of ANs in the network is odd, the transceiver unit for AN_N (marked with the dashed box in Fig. 9) could be removed to support $(N-1)$ ANs. The wavelength assignment is the same as that illustrated in section II and Fig. 2. At each AN, the same B-OADM design, which supports adding one upstream wavelength and dropping one downstream wavelength, as illustrated in section II, could be employed. If more than one wavelength dropping is required at each AN, more than one wavelength dropping filters could be cascaded in series in the B-OADM. The operation principles of the protection switching is the same as that discussed in section II, that is, the switching states of the 2×2 optical switches associated with the affected ANs at the hub node would be automatically toggled, once the fiber failure in the ring network is detected. With this scalable design, the proposed network could be upgraded to support more ANs.

On the other hand, bi-directional in-line optical amplifiers could be employed between adjacent ANs, thus the power budget constraint could be greatly relaxed and more ANs could be supported. With the commercially available Blue/Red filters, which has 18-nm passband at both blue and red bands, and 100-GHz channel spacing AWG, the proposed network could support at least 32 ANs (16 ANs in each band) considering the imperfect passband transition in the Blue/Red filter as well as irrespective of the power budget constraint.

V. Conclusion

We have proposed and demonstrated a single-fiber bidirectional WDM SHR for metro-access network with a hub and multiple ANs. By using the proposed alternate-path switching scheme and the proposed wavelength assignment, the proposed network can provide self-healing function, in case of any single fiber failure in the ring network. No extra protection fiber or any dedicated protection wavelengths is needed. As all the protection switching is performed at the hub only, the operations, administration and management cost can be easily optimized. Thus, the network reliability can be enhanced in a more cost-effective way. Experiment results showed that a fast restoration time of 9 ms could be achieved under a single fiber failure. Design optimization and scalability of the network have been discussed.

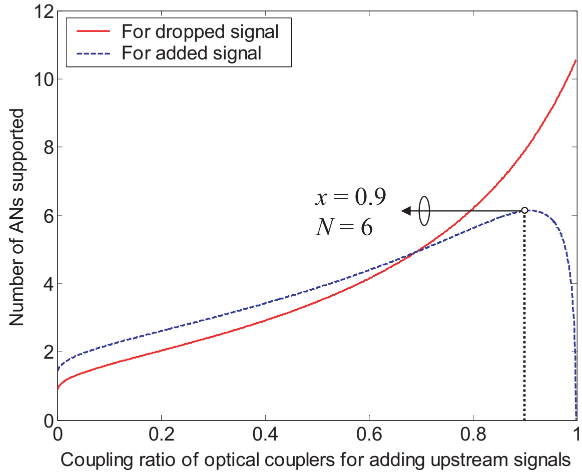

Fig. 8. Number of ANs supported with the optimized coupling ratio of the two optical couplers for adding upstream signals in each AN.

References

[1] T. H. Wu and W. I. Way, "A novel passive protected SONET bidirectional self-healing ring architecture," *IEEE/OSA J. Lightwave Technol.*, vol. 10, no. 9, pp. 1314-1322, 1992.

[2] X. J. Fang, R. Iraschko, and R. Sharma,"All-optical four-fiber bidirectional line-switched ring," *IEEE/OSA J. Lightwave Technol.*, vol. 17, no. 8, pp. 1302-1308, 1999.

[3] H. Hayashi, K. Ohara, H. Tanaka, M. Daikoku, T. Ontani, and M. Suzuki, "Highly reliable optical bidirectional path switched ring applicable to photonic IP networks," *IEEE/OSA J. Lightwave Technol.*, vol. 21, no. 2, pp. 1356-364, 2003.

[4] O. Gerstel and R. Ramaswami,"Optical layer survivability: a services perspective," *IEEE Commun. Mag.*, vol. 38, no. 3, pp. 104-113, March 2000.

[5] A. F. Elrefaie, "Multiwavelength survivable ring network architectures," in *Proc. IEEE International Conference on Communications (ICC) 1993*, vol. 2, pp. 1245-1251.

[6] B. Glance, C. R. Doerr, I. P. Kaminow, and R. Montagne, "Optically restorable WDM ring networks with simple add/drop circuitry," *IEEE/OSA J. Lightwave Technol.*, vol. 14, no. 11, pp. 2453-2456, 1996.

[7] H. Toba, K. Oda, K. Inoue, K. Nosu, and T. Kitoh, "An optical FDM-based self-healing ring network employing arrayed waveguide grating filters and EDFA's with level equalizers," *IEEE J. Sel. Areas Commun.*, vol. 14, no. 5, pp. 800-813, June 1996.

[8] C. H. Kim, C.-H. Lee, and Y. C. Chung, "Bidirectional WDM self-healing ring network based on simple bidirectional add/drop amplifier modules," *IEEE Photon. Technol. Lett.*, vol. 10, pp. 1340-1342, Sept. 1998.

[9] Y. H. Joo, G. W. Lee, R. K. Kim, S. H. Park, K. W. Song, J. Koh, S. T. Hwang, Y. Oh, and C. Shim, "1-fiber WDM self-healing ring with bidirectional optical add/drop multiplexers," *IEEE Photon. Technol. Lett.*, vol. 16, pp. 683-685, Feb. 2004.

[10] S. B. Park, C. H. Lee, S. G. Kang, and S. B. Lee, "Bidirectional WDM self-healing ring network for hub/remote nodes," *IEEE Photon. Technol. Lett.*, vol. 15, pp. 1657-1659, Nov. 2003.

[11] Y. Zhao, X. J. Zhao, J. H. Chen, and F. S. Choa, "A novel bidirectional add/drop module using waveguide grating routers and wavelength channel matched fiber gratings," *IEEE Photon. Technol. Lett.*, vol. 11, no. 9, pp. 1180-1182, 1999.

[12] F. Bilodeau, D. C. Johnson, S. Theriault, B. Malo, J. Albert, and K. O. Hill, "An all-fiber dense wavelength division multiplexer/demultiplexer using photoimprinted Bragg gratings," *IEEE Photon. Technol. Lett.*, vol. 7, no. 4, pp. 388-390, 1995.

[13] X. F. Sun, Z. X. Wang, C. K. Chan, C. L. Lin, and L. K. Chen, "A single-fiber bi-directional self-healing WDM metro-ring network with bi-directional OADM," in *Proc. European Conference on Optical Communications (ECOC) 2005*, paper We4.P.41.

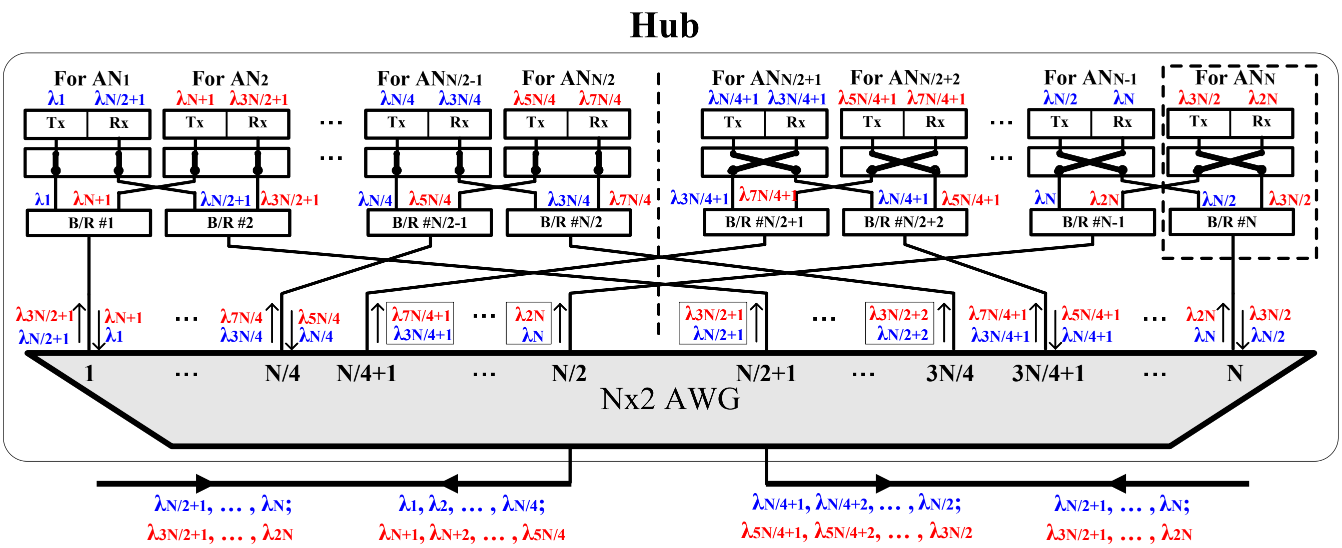

Fig. 9. Configuration of the hub node with N ANs in the proposed network under normal operation. Note: the upstream wavelength channels marked with boxes are the working ones; while those without boxes will be blocked by their respective destined transmitters.

[14] R. J. S. Pedersen and B. F. Jorgensen, "Impact of coherent crosstalk on usable bandwidth of a grating-MZI based OADM," *IEEE Photon. Technol. Lett.*, vol. 10, pp. 558-560, April 2003.

Xiaofeng Sun (S'04) received the B.Sc. degree in Electronic Engineering from the Tsinghua University, Beijing, China, in 2003 and the M.Phil. degree in Information Engineering from the Chinese University of Hong Kong in 2006. Currently, he is working as a consultant at Norson Telecom Consulting, which is a Beijing-based consulting firm providing research and consulting services on China's telecom market. His research interests include optical communications and optical access networks.

Chun-Kit Chan (S'93–S'95–M'97–SM'04) received the B.Eng., M.Phil., and Ph.D. degrees from The Chinese University of Hong Kong, Hong Kong, all in information engineering. In 1997, he joined the Department of Electronic Engineering, City University of Hong Kong, as a Research Assistant Professor. In 1999, he joined Bell Laboratories, Lucent Technologies, Holmdel, NJ, as a Member of Technical Staff, where he worked on control of widely tunable semiconductor lasers and realization of an optical packet switch fabric with terabit-per-second capacity. In August 2001, he joined the Department of Information Engineering, CUHK, where he is currently an Associate Professor. He has served as the member of the technical program committee for OFC/NFOEC from 2005-2007 and other international conferences. He has published more than 150 technical papers in refereed international journals and conference proceedings and holds one issued U.S. patent. Currently, he serves as the Associate Editor of *OSA Journal of Optical Networking*. His main research interests include optical access networks, optical packet switching, and optical performance monitoring.

Zhaoxin Wang (S'04) received the B.Sc. and M.Sc degrees in Electronic Engineering from the Tsinghua University, Beijing, China, in 2000 and 2003, respectively; and the Ph.D. degree in Information Engineering from the Chinese University of Hong Kong in 2006. Currently, he serves as a Member of Professional Staff at the Hong Kong Applied Science and Technology Research Insititute (ASTRI). His research interests include optical signal processing and optical access networks.

Chinlon Lin (S'71–M'73–SM'79–F'91) received his BSEE from National Taiwan University in 1967, began his study in the US in 1968, and received his MS in 1970 from University of Illinois, and a Ph. D. from Univ. of California, Berkeley, in 1974. At UC Berkeley he was a recipient of an IBM Graduate Fellowship and a Lankersheim Scholarship.

He joined AT&T Bell Labs' Laser Sciences Research Department, Communication Sciences Research Division, Holmdel, NJ, in 1974. At Bell Labs, his research included studies of nonlinear optics in fibers, self-phase-modulation, tunable infrared fiber Raman lasers, fiber Raman amplifiers and four-wave-mixing for optical frequency conversion, as well as dynamic optical frequency chirp studies in high-speed semiconductor laser modulation for high-bit-rate fiber transmission systems. He originated and demonstrated the first idea of both dispersion-shifted fibers and dispersion-compensating fibers that became the ubiquitous fiber infrastructure of today's long-haul high-speed fiber transmission systems and in global undersea optical fiber networks. He received an IEE Electronics Letters Premium award for the work on dispersion-shifted fibers (DSF), and also was granted a US patent on the idea of dispersion-compensating fibers (DCF). In 1984 he was on leave from Bell Labs as a Visiting Guest Professor at the Tech. Univ. of Denmark.

He joined Bellcore (Bell Communications Research) in 1986 where he was Director of Broadband Lightwave Systems Research. He led a group working on the broadband optical access architectures and technologies such as FTTH, FTTC, HFC systems, DWDM tunable filters and EDFAs for high-capacity digital and analog video systems, and lightwave systems for multi-channel hybrid AM/QAM-digital video distribution for HFC networks. He joined Tyco Submarine Sys. R & D Labs (formerly AT&T Submarine Systems) in September 1997, to work on DWDM global long-haul undersea fiber networks. In May 2000 he founded Jedai Broadband Networks, a startup to work on Fiber-to-the Business high-speed access solutions for cable TV industry. In January 2003 he joined CUHK as Professor of Photonics and Director of IOSAT (Institute of Optical Science and Technology) and the Center for Advanced Research in Photonics, and is a Professor of both EE and IE departments.

He has published over 180 papers and conference presentations, several invited book chapters and 12 patents. He was an Assoc. Editor for *IEEE Journal of Lightwave Technology* and *IEEE Photonics Technology Letters* and was on the technical program committees for OFC, Optical Amplifier Topical Meeting, Topical Meeting on Optical Networking, etc. Recently he was also on the technical program committee for European Conference on Optical Communications (ECOC) conferences from 2004-2006. He has edited two books, the recent one being *Broadband Optical Access Networks and Fiber-to-the Home* (Wiley, August 2006).

He is a Fellow of both IEEE and OSA, and also the Photonics Society of Chinese Americans, of which he also served as President in 1994.

Lian-Kuan Chen (S'86–M'92–SM'04) received his BS degree from National Taiwan University in 1983 and MS and PhD degree from Columbia University in 1987 and 1992 respectively, all in electrical engineering. He worked at Jerrold Communications, General Instruments (GI), USA in 1990-1991 and engaged in research on linear lightwave video distribution systems, with contributions on the distortion reduction schemes for various optical components. He joined the Department of Information Engineering, the Chinese University of Hong Kong in 1992 and established the Lightwave Communications Laboratory. He has been the Head of Department in 2004-06. His current research interests include broadband local access networks, photonic signal processing, and the performance monitoring and fault management of optical networks. He is grateful that most of the projects are supported by the research grants of Hong Kong SAR government. He has published more than 180 papers in international conferences and journals, primarily in the field of optical communications. Currently he serves as the Associate Editor of *IEEE Photonics Technology Letters*.